Soil Moisture Wireless Sensing with Analog Scatter Radio, Low Power, Ultra-Low Cost and Extended Communication Ranges

Spyridon Nektarios Daskalakis, Stylianos D. Assimonis, Eleftherios Kampianakis and Aggelos Bletsas
School of Electronic and Computer Engineering, Technical Univ. of Crete, Chania, Greece 73100
sdaskalakis@isc.tuc.gr, assimonis@telecom.tuc.gr, ekabianakis@isc.tuc.gr, aggelos@telecom.tuc.gr

***Abstract*—The measurement of the soil moisture is critical in agriculture. In this work a joint analog design of wireless transmitter with scatter radio and capacitive sensor for soil moisture is presented. The design is based on a custom microstrip capacitor, exploits bistatic analog scatter radio principles and is able to wirelessly convey soil moisture percentage by mass (% MP) with RMS error of 1.9%, power consumption and communication range on the order of 100 uWatts and 100 meters, respectively. It is tailored for ultra-low cost (5 Euro per sensor) agricultural sensor network applications for soil moisture.**

I. Introduction

Dense soil moisture sensing could vastly improve irrigation systems and offer tremendous water savings. Novel soil moisture capacitive sensors have appeared in the literature, typically integrated with a discrete wireless radio module [1], or a discrete processing chip [2], including inkjet fabrication designs of the sensing element. In an effort to achieve extended wireless communication ranges, while reducing the monetary and energy cost, recent work [3], [4] proposed a joint-design of environmental relative humidity sensing. The wireless communicator, based on analog scatter radio, simplifying the radio front-end to a single transistor. Instead of environmental relative humidity, this work offers an improved joint-design of scatter radio and capacitive sensor for soil moisture agricultural wireless networks. The target goal of this work is a soil moisture percentage (%SM) wireless sensor network with extended ranges, low power and cost.

The analog backscatter node consists of an antenna, a control circuit and the radio frequency (RF) front-end between them (Fig. 1). The control circuit alternates with a specific frequency, $F_{\rm sw}$, the termination load of the antenna through a signal which controls the "ADG919" switcher. The latter is located at the RF front-end area. The different termination loads, Z_1 and Z_2, offer different reflection coefficient, Γ_1 and Γ_2, respectively, according to,

$$\Gamma_{\rm i} = \frac{Z_{\rm i} - Z_{\rm a}^*}{Z_{\rm i} + Z_{\rm a}^*}, \tag{1}$$

with ${\rm i} = 1, 2$, $Z_{\rm a}$ the antenna impedance. Two typical reflection coefficients are depicted in Fig. 1 (down, left). Hence, when a signal with carrier frequency, $F_{\rm c}$, impinges on the sensor node, frequency modulation occurs and the reflected signal on frequency domain is depicted in Fig. 1 (down, right). Finally,

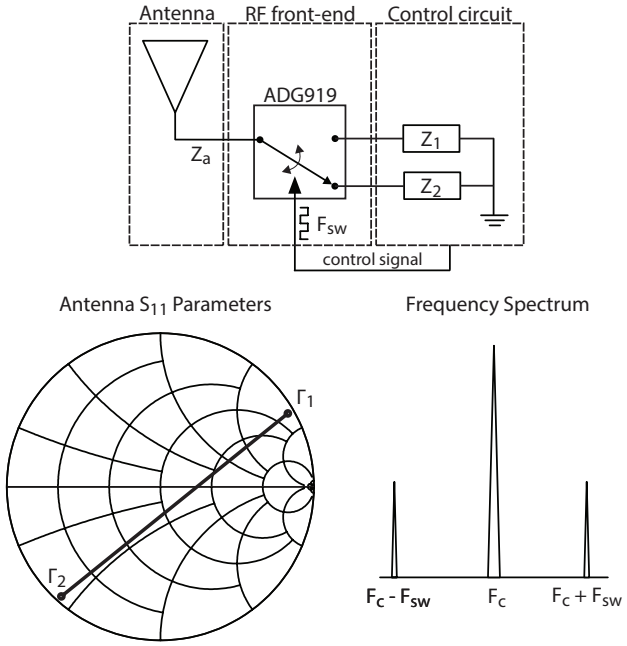

Fig. 1: Scatter radio communication principles: The low power RF switch "ADG919" alternates the termination loads (Z_1 and Z_2) of the antenna with frequency $F_{\rm sw}$. When a carrier is equal with frequency $F_{\rm c}$, two subcarriers appear, with frequencies $F_{\rm c} \pm F_{\rm sw}$.

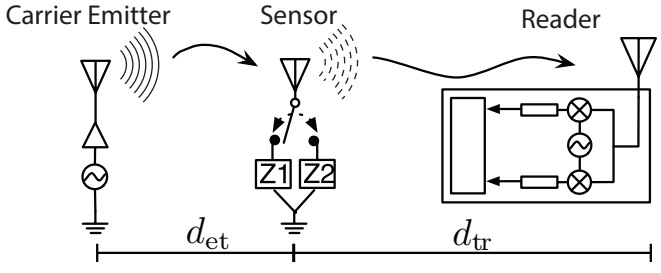

Fig. 2: Bistatic backscatter sensor network architecture. Low-cost emitter produce the carrier signal which is modulated by sensor nodes and finally, the reflected signal is received by a software defined radio (SDR) reader.

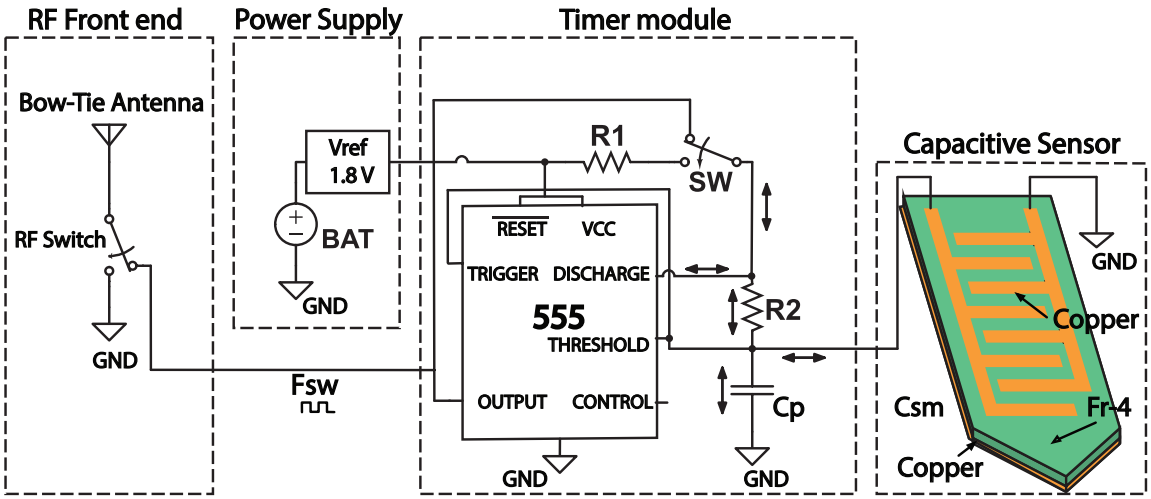

Fig. 3: Analog backscatter sensor node schematic.

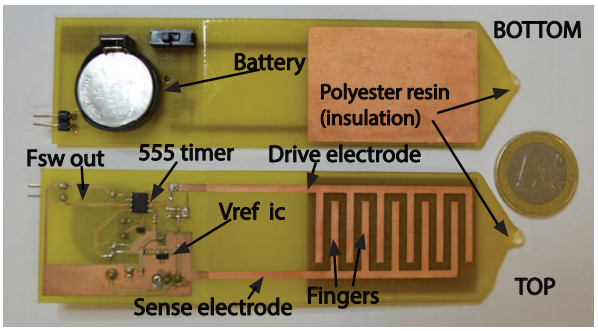

Fig. 4: Fabricated circuit board with capacitive sensor, power supply circuit and timer module circuit.

the obtained subcarriers are

$$F_{\text{sub,1}} = F_{\text{c}} + F_{\text{sw}}, \tag{2}$$
$$F_{\text{sub,2}} = F_{\text{c}} - F_{\text{sw}}. \tag{3}$$

Different F_{sw} leads to different $F_{\text{sub,i}}$. On the other hand, the F_{sw} can be affected by the soil moisture with a specific way, which will be explained below.

The RF front-end was designed according to [4] in order to maximize the communication efficiency. The RF switch "ADG919" was chosen due to its low insertion loss (0.8 dB at 1 GHz) and high isolation (43 dB at 1 GHz). The antenna was a low-cost microstrip (FR-4) bow-tie antenna designed at 868 MHz, which is the center frequency of the UHF ISM-band in Europe.

Finally, the bistatic scatter radio topology was implemented, as shown in Fig. 2. The carrier emitter, which was a portable simple pulse generator with an amplifier, was placed in a different location from the reader, which was a commercial software defined radio (SDR). The carrier emitter-to-node and the reader-to-node distance is d_{et} and d_{tr}, respectively (Fig. 2).

II. Implementation

The analog backscatter node equivalent circuit is depicted in Fig. 3. The monolithic timer "CSS555" from Custom Silicon Solutions was set up in astable multi-vibrator mode, playing the role of the *capacitance-to-frequency* (CtF) converter. The timer is connected to a resistor-capacitor (R_1, R_2, C_{p}, C_{sm}) network including the fabricated microstrip capacitive sensor C_{sm} (Fig. 3,4). The capacitor has two electrodes (drive and sense) and was designed on FR-4 substrate (thickness 1.5 mm, $\epsilon_{\text{r}} = 4.6$). Finally polyesterresin was used for waterproofing. When the capacitive sensor is placed into the soil, the %SM affects the capacitance C_{sm}. High soil moisture leads to high capacitance. Next, the C_{sm} affects the obtained frequency F_{sw} from the timer and the corresponding $F_{\text{sub,i}}$, as a result. Hence, different %SM produce different F_{sub} and frequency modulation occurs.

According to Fig. 3, the parallel capacitors (C_{p} and C_{sm}) are periodically charged and discharged (arrows in Fig. 3) through resistors R_1 and R_2, producing square wave pulses with frequency,

$$F_{\text{sw}} = \frac{1}{\ln(2)\ (R_1 + 2R_2)\ (C_{\text{p}} + C_{\text{sm}})}, \tag{4}$$

while the duty cycle of the produced wave is,

$$D = \frac{R_1 + R_2}{R_1 + 2R_2}. \tag{5}$$

According to [5], the duty cycle is related to the fundamental subcarrier frequency power of the scattered signal. More specifically, the power will increased as D is close to 50%. Hence, according to (5), $R_1 = 0$ when $D = 0.5$. On the other hand, if $R_1 = 0$ there is power leakage at "DISHARGE" pin. Consequently, in this work D was fixed at 60%. Thus, from (5), $R_1 = R_2/2$.

Many of the above backscatter nodes can operate simultaneously, using frequency division multiple access (FDMA). Fig. 6 depicts the obtained subcarriers of four sensor nodes and the carrier at 868 MHz. Each node i uses a unique spectrum band. The bandwidth limits depend on the lowest

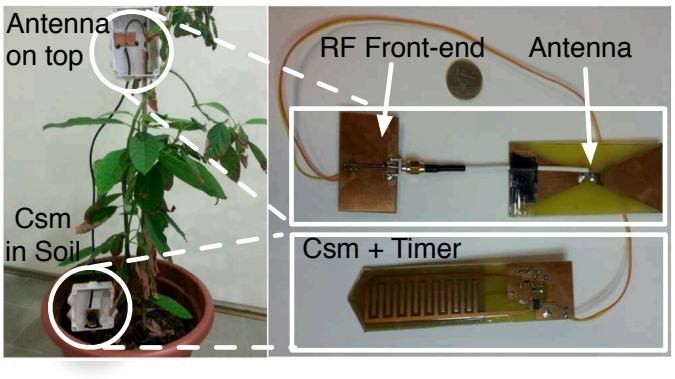

Fig. 5: Left: Installation of the sensor on an avocado plant with utilization of "IP65"-rated enclosures. Right: Close-up view of the fabricated sensor

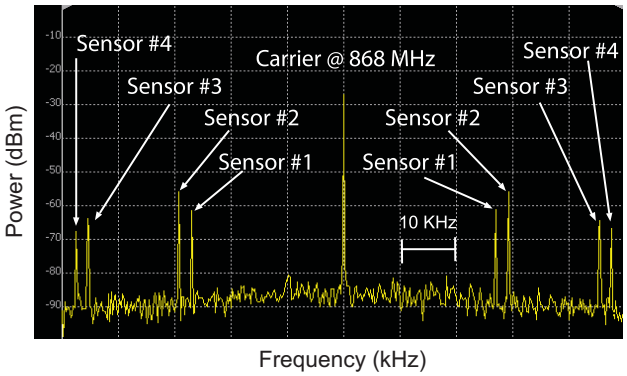

Fig. 6: Sensor network spectrum for sensors 1, 2, 3, 4. Sensors 1, 2 and 3, 4 occupy a bandwidth of 1 and 5 kHz, respectively.

($F^{\mathrm{L}}_{\mathrm{sw,i}}$) and highest frequency ($F^{\mathrm{H}}_{\mathrm{sw,i}}$), which is produced by the timer module when the %SM is 100 and 0, respectively. Assuming that a sensor uses bandwidth B_{i} and C_{L}, C_{H} are the C_{sm} capacitance for 0, 100 %SM, respectively, the $C_{\mathrm{p,i}}$ and R_{i} at i-th node is,

$$C_{\mathrm{p,i}} = \frac{B_{\mathrm{i}}\ C_{\mathrm{L}} + F^{\mathrm{L}}_{\mathrm{sw,i}}\ (C_{\mathrm{H}} - C_{\mathrm{L}})}{B_{\mathrm{i}}}, \tag{6}$$

$$R_{1,\mathrm{i}} = \frac{1}{2} R_{2,\mathrm{i}} = \frac{B_{\mathrm{i}}}{3\left(\ln(2)\ F^{\mathrm{L}}_{\mathrm{sw,i}}\ (C_{\mathrm{H}} - C_{\mathrm{L}})\ (F^{\mathrm{L}}_{\mathrm{sw,i}} + B_{\mathrm{i}})\right)}. \tag{7}$$

III. Experimentation and Results

Four nodes were fabricated in-house in order to evaluate the proposed system. At each backscatter sensor node the bow-tie antenna with the RF front-end was located well above the ground, while the fabricated capacitor was placed into the soil. The connection between the switch and the timer was established via shielded coaxial cables (Fig. 5). The ultra-low power consumption of 55.5 uA at 1.8 V (100 μW), provides a lifetime of 10.4 months of continuous (not duty-cycled) operation with the utilization of a 300 mAh "CR2032" battery. Multiple access was implemented with the aforementioned FDMA scheme so that each sensor node occupied a unique

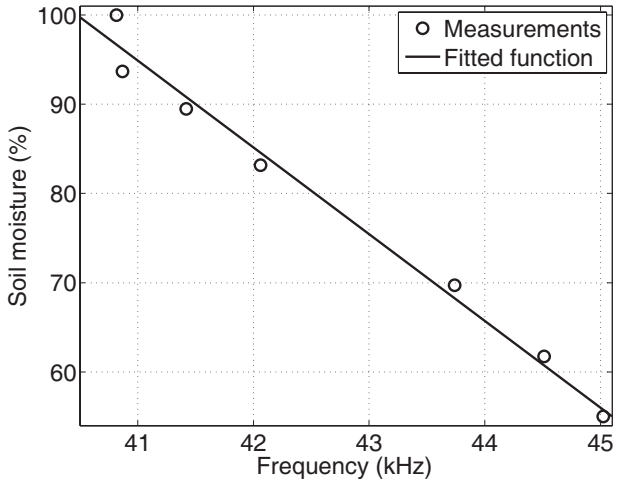

Fig. 7: Measured soil moisture (%) characteristic and fitted function versus frequency.

spectrum band. There is a 1 KHz band-gap between the bandwidth of each sensor in order to avoid the adjacent channel interference between the $F^{H}_{sw,i}$ and $F^{L}_{sw,i+1}$ signals of i-th and (i+1)-th node. This was implemented by installing the corresponding passive components according to (6), (7) on each sensor node.

A calibration procedure was utilized in order to convert the frequency output of the sensor nodes to the corresponding %SM. Calibration involves monitoring the nodes' output for various %SM values and calculating the corresponding transfer function using polynomial fitting. A sample of soil was dried and weighted in order to emulate different %SM conditions. Specific amount of water was poured and the %SM was calculated by,

$$\%\mathrm{SM} = \frac{M_{\mathrm{W}} - M_{\mathrm{D}}}{M_{\mathrm{D}}}, \tag{8}$$

where M_{W} and M_{D} is the mass of the wet and dried soil sample, respectively. Fig. 7 depicts the transfer function and the %SM samples from a node for a soil moisture value of 55-95 %. It is prominent that frequency is almost a linear function of %SM. The subcarrier frequency data, collected during the calibration procedure (1500 samples), were input into the transfer function in order to characterize the measurement accuracy of the nodes. The %SM output of the transfer function was compared with the reference measurements. It was found that the nodes exhibit a root mean squared error (RMSE) and a mean absolute error (MAE) of 0.1 %SM and 0.08 %SM, respectively, which is sufficient for precision agriculture.

A setup, which consists of a receiver implemented on a commodity SDR platform, a node operating at 28.5 kHz and an emitter which produced a carrier wave (CW) with 20 mW power, was utilized in order to investigate the backscatter nodes' communication performance. The equipment was set up in bistatic topology with $d_{\mathrm{et}} = 7.5$ m and $d_{\mathrm{tr}} = 100$ m. The frequency value of the sensor was monitored using a data-logger and it was compared with the corresponding estimated

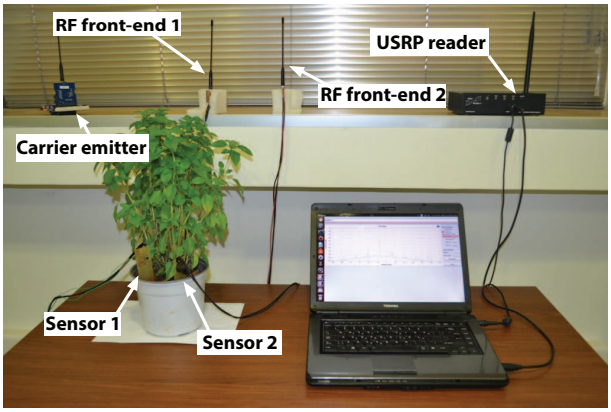

Fig. 8: Indoor setup testbed of the bistatic analog backscatter architecture.

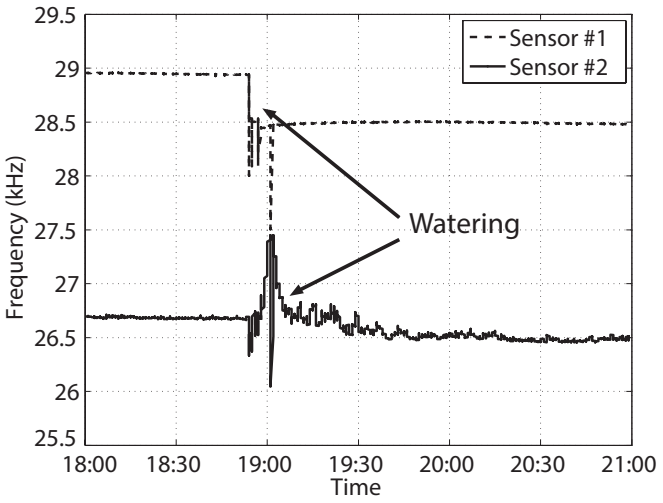

Fig. 9: Soil moisture measurements of two sensors for 3 hours.

TABLE I: Example with two sensor nodes.

Sensor #	R_1(kΩ)	R_2 (kΩ)	D(%)	F_{sw}	P_{tot} (μW)
1	8.8	17.6	60	28.5	58.6
2	7.4	14.7	60	26.5	66.8

frequency at the reader. An RMSE of 1.9 %SM was observed for a dataset of 1500 samples.

Moreover a testbed with two sensor nodes was installed in a basil plant in the lab (Fig. 8). The frequency data that was collected for a period of 3 hours are illustrated in Fig. 9. It is observed that after the watering instance, the output frequency of the nodes changes instantly, while it settles after approximately 20 minutes. Table I contains the specifications of the sensors including the corresponding resistor values, frequency pulse's duty cycle, center frequency value and power consumption. The cost of each sensor in quantities of 1 is 5 Euro (the SMA connector is not included in the price, since the antenna will be integrated with the RF front-end in future designs).

IV. Conclusion

This work develops a soil moisture sensor network node that costs 5 Euro and consumes power on the order of 100 μW. The backscatter sensor nodes consists of a CtF implemented with a 555 timer that is connected to a custom capacitive soil moisture sensing element. Soil moisture is frequency modulated and the voltage pulses of the converter are driven to the single-switch RF front-end that implements scatter-radio communication. The scattered signals are received by the SDR reader that converts frequency to %SM via a carefully calculated calibration function. Soil moisture is measured by the nodes with an RMSE and MAE on the order of 0.1 and 0.08 %SM respectively.

For communication range of d_{et}=7.5 m and d_{tr}=100 m the RMSE is on the order of 1.9 %SM. For the networking capability, the sensors utilize an FDMA scheme that is implemented via the installation of specific passive components on each node. Future work will focus on developing and deploying an ultra large scale network of such sensor nodes.

Acknowledgment

This work was supported by the ERC-04-BLASE project, executed in the context of the Education & Lifelong Learning Program of General Secretariat for Research & Technology (GSRT) and funded through European Union-European Social Fund and national funds.

References

[1] Y. Kawahara, H. Lee, and M. M. Tentzeris, "Sensprout: inkjet-printed soil moisture and leaf wetness sensor," in *ACM Conf. on Ubiquit. Comp.*, Sept. 2012, pp. 545–545.

[2] S. Kim, Y. Kawahara, A. Georgiadis, A. Collado, and M. Tentzeris, "Low-cost inkjet-printed fully passive rfid tags using metamaterial-inspired antennas for capacitive sensing applications," in *IEEE MTT-S Int. Microw. Symp. Dig.*, Jun. 2013, pp. 1–4.

[3] E. Kampianakis, J. Kimionis, K. Tountas, C. Konstantopoulos, E. Koutroulis, and A. Bletsas, "Wireless environmental sensor networking with analog scatter radio and timer principles," *IEEE Sensors J.*, accepted for publication.

[4] S. D. Assimonis, E. Kampianakis, and A. Bletsas, "Microwave analysis and experimentation for improved backscatter radio," in *IEEE Europ. Conf. on Antennas and Prop.*, Apr. 2014.

[5] S. W. Smith, *The scientist and engineer's guide to digital signal processing*. California Technical Publishing, San Diego, 1997.